Polish Society of Composite Materials
Polskie Towarzystwo Materiałów Kompozytowych

19: 1 (2019) 7-13

COMPOSITES THEORY AND PRACTICE
ISSN: 2084-6096
ISSN (online): 2299-128X

Iwona Sulima, Paweł Hyjek, Piotr Malczewski

Pedagogical University of Cracow, Institute of Technology, ul. Podchorążych 2, 30-084 Cracow, Poland
**Corresponding author. E-mail: iwona.sulima@up.krakow.pl*

Received (Otrzymano) 14.12.2018

THE TRIBOLOGICAL PROPERTIES OF SINTERED STEEL-MATRIX COMPOSITES

The tribological properties of composite materials reinforced with titanium diboride were investigated. Abrasion resistance tests were carried out at room temperature in a ball-on-disc system. Balls with a diameter of 3.14 mm were used as the counter-samples. The effect of the TiB_2 content and counter-sample material (Al_2O_3, Si_3N_4, ZrO_2, AISI52100 steel) on the coefficient of friction and wear rate of the sintered composites and 316L steel was determined. After the abrasion tests the sample surfaces were examined by scanning electron microscopy. The obtained results show that the tribological properties depend on the test conditions and content of the TiB_2 reinforcing phase.

Keywords: **tribological properties, friction coefficient, composites, titanium diboride (TiB_2)**

WŁAŚCIWOŚCI TRIBOLOGICZNE KOMPOZYTÓW NA OSNOWIE STALOWEJ

W pracy przedstawiono właściwości tribologiczne materiałów kompozytowych wzmacnianych dwuborkiem tytanu. Badania odporności na zużycie przeprowadzono w temperaturze pokojowej w skojarzeniu kulka-tarcza. Jako przeciwpróbki użyto kulki o średnicy 3,14 mm. Określono wpływ ilości TiB_2 i materiału przeciwpróbki (Al_2O_3, Si_3N_4, ZrO_2, stal AISI52100) na współczynnik tarcia oraz zużycie spiekanych materiałów kompozytowych i stali 316L. Powierzchnie próbek po testach tribologicznych obserwowano za pomocą skaningowego mikroskopu elektronowego. Uzyskane wyniki badań wykazały, że na właściwości tribologiczne wpływają warunki badań i ilość fazy wzmacnianej TiB_2.

Słowa kluczowe: **właściwości tribologiczne, współczynnik tarcia, kompozyty, dwuborek tytanu (TiB_2)**

INTRODUCTION

Powder metallurgy is an effective and competitive technology to manufacture finished products from metals, ceramics and composites with very diverse properties [1, 2]. An important group of materials produced by powder metallurgy includes metal matrix composites dispersion-strengthened with particles, or with continuous and discontinuous (discrete) fibres [3-5]. The use of powder metallurgy to manufacture metal matrix composites enables a diffusion bond to be produced between the matrix and the reinforcement. It also offers vast possibilities in choosing the type, form and size of the reinforcing phase and allows products with the same chemical composition to be made, but with different values of density. Literature data [6-9] indicates a high level of interest in composites based on iron alloys reinforced with ceramic particles. The main reason for this interest is the low cost of steel production and high mechanical properties of the composites, additionally combined with satisfactory corrosion resistance. The ceramic phase introduced into the steel matrix improves the mechanical properties and wear resistance of the composites [10-13]. Among various ceramic materials, titanium boride is considered to be one of the best reinforcements for the steel matrix due to its high melting temperature (3225°C), low density (4.5 g/cm^3), outstanding tribological properties and good compatibility with this matrix. TiB_2 ceramic materials are characterized by high hardness (3400 HV) and high corrosion resistance at temperatures up to 1400°C, high temperature chemical and structural stability, and resistance to thermal shock [14-16].

Tribological properties are important characteristics of structural materials. According to the definition, tribological wear is a kind of surface wear caused by friction processes. Under conditions of dry friction, abrasive wear is the dominant process [17]. The abrasive wear of composite materials depends on the morphology and volume fraction of the reinforcing phases, and also on the type, distribution and properties of these phases. The second group of factors responsible for the abrasive wear of composites includes the test conditions such as load, rotational speed, displacement, test temperature, counter-sample material, and the test environment [17-20]. According to the literature [8, 21, 22], studies were carried out to ascertain the impact of TiB_2 on the tribological properties of stainless steels. Tjong and Lau [21] used a pin-on-disc system to investigate the tribological properties of composites based on 304 steel with 20 vol.% TiB_2. The tests were carried out under different loads (15, 35 and 55 N) and at different speeds (1÷3 m/s). The results showed that the volumetric wear of the composite decreased with increasing the load or speed. It was observed that during the tribological tests, fragmentation (breakdown) of the TiB_2 particles into smaller pieces occurred. In another research work, Tjong and Lau [22] determined the abrasion resistance of sintered steel matrix composites with varying contents of TiB_2 ceramics. It was demonstrated that adding TiB_2 to the matrix significantly improved the abrasion resistance of the composite. Regardless of the test conditions used, the abrasion resistance of the composites containing ≥10 vol.% TiB_2 was ten times higher compared to the abrasion resistance of sintered 304 steel without the reinforcing phase.

METHODS

The raw materials used in this research were 316L austenitic stainless steel and 316L steel matrix composites containing 5 vol.% TiB_2 and 10 vol.% TiB_2. The materials were sintered using Spark Plasma Sintering (SPS/FAST). The sintering process was carried out at the pressure of 35 MPa and temperature of 1100°C for 5 minutes.

The density of the composites was measured by the Archimedes method. The Young's moduli of the composites were measured by ultrasound to determine the transverse and longitudinal wave velocity using the ultrasonic flaw detector Panametrics Epoch III. The phase constituents and the microstructures of the specimens were analyzed by X-ray diffraction (XRD, Brucker Discover D8) operating with Cu K_α radiation and scanning electron microscopy (SEM, JEOL JSM 6610LV) equipped with energy dispersive spectroscopy (EDS). Vickers microhardness measurements using a load of 2.94 N were carried out with a NEXUS 4000 hardness tester. Ten replicate tests were conducted and the mean value was given.

Before the tribological tests, the surfaces of the investigated materials were prepared in accordance with norm [23]. The samples for the tribological tests were prepared by standard methods of grinding using SiC foil and polishing up to 0.4 μm using a diamond suspension. Prior to the tribological tests, all the specimen surfaces were cleaned with alcohol and dried. The surface roughness of the specimens was below 0.2 μm (R_a). The wear properties of the sintered materials were examined using a ball-on-disc machine under dry friction conditions. The tribological test consists in gradual removal of a certain volume of material when two samples, i.e. a fixed ball and a rotating disc, are rubbing against each other loaded with a constant force. As a result of this process, a toroidal groove (track) is formed on the disc surface [24]. The tribological tests were conducted using four types of balls (steel AISI52100, Al_2O_3, Si_3N_4, ZrO_2), two volume percentages of TiB_2 (5 and 10 vol.%), and at constant normal loads of 5 N, sliding distance of 1000 m and sliding velocity of 0.1 m/s. In the tests described in this article, balls with a diameter of 3.175 mm were used and parameters such as coefficient of friction μ, the weight loss and the specific wear rate coefficient were determined. The accuracy of the weight is 0.1 mg. The accuracy of measuring the friction force is 0.2%. For each sintered material, three tribological tests were carried out. Table 1 gives the conditions and parameters under which the tribological tests were carried out by the ball-on-disc method. The friction coefficient was calculated from the following equation [23]:

$$\mu = \frac{F_f}{F_n} \tag{1}$$

where: F_f - measured friction force [N], F_n - applied normal force [N].

The specific wear rate according to the wear volume was calculated by means of equation (2) [23]:

$$W_{V(disc)} = \frac{V_{disc}}{F_n \cdot L} \tag{2}$$

where: $W_{V(disc)}$ - specific wear rate of the disc [mm^3/Nm], V_{disc} - wear volume of the disc specimen [mm^3], F_n - applied load [N], L - sliding distance [m].

After testing, the worn surfaces were investigated using Scanning Electron Microscope (JEOL JSM 6610LV).

TABLE 1. **Tribological test conditions using ball-on-disc method**

TABELA 1. **Warunki testów tribologicznych przy użyciu metody ball-on-disk**

Tribological test conditions	
temperature	23°C
ball types	Al_2O_3, Si_3N_4, ZrO_2, steel AISI52100
ball diameter d	3.175 mm
normal load F_n	5 N
friction track diameter r	5.0 mm
sliding speed v	0.1 m/s
total sliding distance L	1000 m
test duration t	10000 s

RESULTS

Figure 1a shows the microstructure of the 316L steel+10%TiB_2 composites. The microstructure of the composites is characterized by uniform distribution of the reinforcing TiB_2 phase (black areas) along the grain boundaries in the steel matrix. The X-ray diffraction studies (Fig. 1b) of the composites confirmed the presence of TiB_2 particles, while the X-ray diffraction phase analysis of the matrix revealed some peaks derived from austenite (γ).

a)

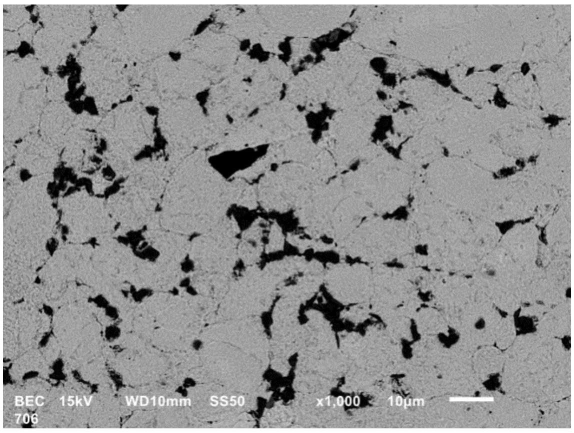

b)

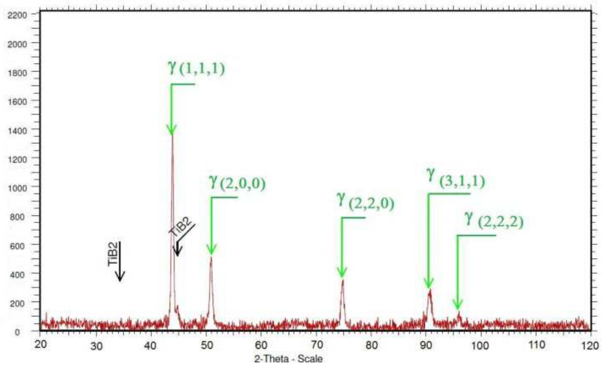

Fig. 1. Selected micrograph before tribological test (a) and X-ray diffraction pattern of 316L steel+10TiB_2 composites (b)

Rys. 1. Przykładowa mikrostruktura przed testami tribologicznymi (a) oraz dyfraktogram kompozytu stal 316L+10% TiB_2 (b)

Table 2 compares selected physical and mechanical properties of the sintered composites and sintered 316L austenitic steel without the reinforcing phase. All the materials sintered by the SPS/FAST method were characterized by a high degree of consolidation. For these materials, a high density reaching 97÷99% of the theoretical density was obtained. A change in the Young's modulus was observed with increasing the content of titanium diboride. For the steel without the reinforcement, the value of Young's modulus was 191 GPa and it increased to 227 GPa for the 316L steel+10% TiB_2 composite. The results of the microhardness tests showed a similar relationship. The microhardness of the sintered composites grew with increasing the TiB_2 content. The highest microhardness (475 HV 0.3) was obtained for the 316L steel+10% TiB_2 composite (Table 2).

Figure 2 shows the variations in the coefficient of friction of the sintered materials with increasing the test duration. Table 3 presents the collective results of the tribological tests carried out on 316L austenitic steel and the composites sintered by the SPS method. From the obtained results of abrasion resistance tests, it follows that the coefficient of friction depends on the content of reinforcing phase in the steel matrix, and it decreases with increasing the TiB_2 content in this matrix. A comparative study showed that the lowest coefficient of friction was obtained by the 316L steel+10%TiB_2 composites.

TABLE 2. **Selected properties of sintered steel and composites**

TABELA 2. **Wybrane właściwości spiekanej stali 316L i kompozytów**

Sintered materials	Apparent density ρ_0 [g/cm^3]	[%]	Young's modulus E [GPa]	[%]	Microhardness HV0.3
316L steel	7.91±0.03	99	191±3	92	225±5
316L steel+5%TiB_2	7.51±0.03	99	215±3	95	396±8
316L steel+10%TiB_2	7.08±0.03	97	227±3	94	475±9

The coefficient of friction assumes different values depending on the type of counter-sample used (Al_2O_3, Si_3N_4, ZrO_2 and AISI52100 steel). The highest values of this coefficient, i.e. 0.70, 0.62 and 0.59, were obtained for the 316L steel, 316L steel+5%TiB_2 composite and 316L steel+10%TiB_2 composite, respectively, when the counter-sample made of AISI52100 steel was used in the tests. The lowest values of the coefficient were obtained by the sintered composites and Al_2O_3 used as the counter-sample in the tests (Table 3, Fig. 3).

Compared to 316L steel without reinforcement, introducing the reinforcing phase into the steel matrix reduces the wear rate of the composites (Fig. 4). For example, in the tests with the Al_2O_3 counter-sample, the mass loss and specific wear rate ($W_{s(disc)}$) obtained for 316L steel were 0.0319 g and $823.23\cdot10^{-6}$ mm^3/N·m, respectively. For the composite materials with 10 vol.% TiB_2, the mass loss and the wear rate were 0.0171 g and $482.37\cdot10^{-6}$ mm^3/N·m, respectively. This demonstrates the higher wear resistance of the 10 vol.% TiB_2 composites. The titanium diboride particles protect the steel matrix during friction, reducing its wear. In the composites containing 10 vol.% TiB_2, the removal of material was less severe. The same trend was observed in other samples subjected to tribological tests carried out with the counter-samples made of AISI52100 steel, Si_3N_4 and ZrO_2.

From the results of the tribological tests, it follows that the highest values of wear rate were obtained for the 316L steel and the composites tested for abrasion resistance with the Al_2O_3 balls. On the other hand, the lowest values of wear rate were obtained during tests using the steel balls. A similar tendency was observed in the relationship between the mass loss and type of counter-sample used. Differences in the obtained values of the mass loss and wear rate might be due to differences in the hardness of the material used for the counter-sample. According to literature data, the hardness of Al_2O_3, Si_3N_4, ZrO_2 and steel is 2200 HV, 2100 HV, 1300 HV and 850 HV [25, 26], respectively. The friction ball made of Al_2O_3 is characterized by the highest hardness, hence it can easily penetrate the material and remove it from the surface exposed to wear.

a)

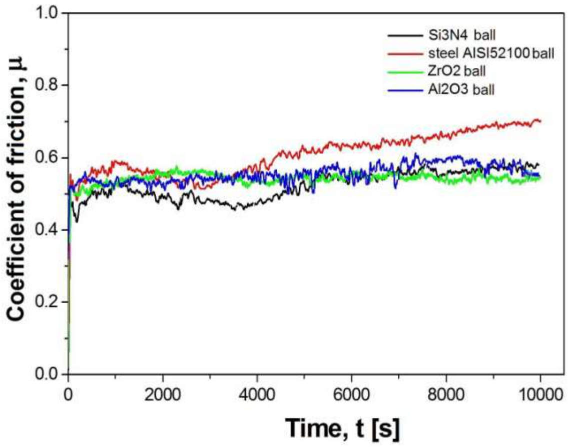

b)

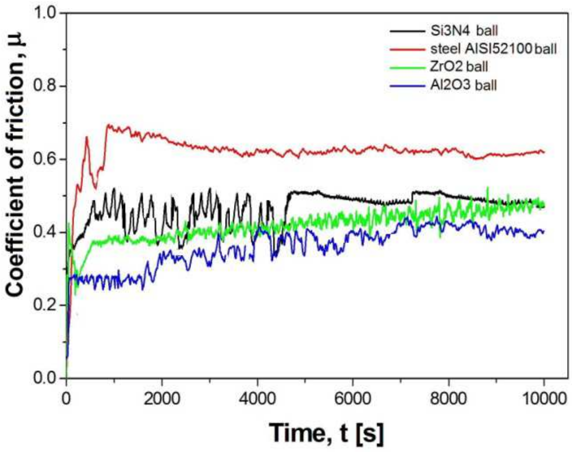

c)

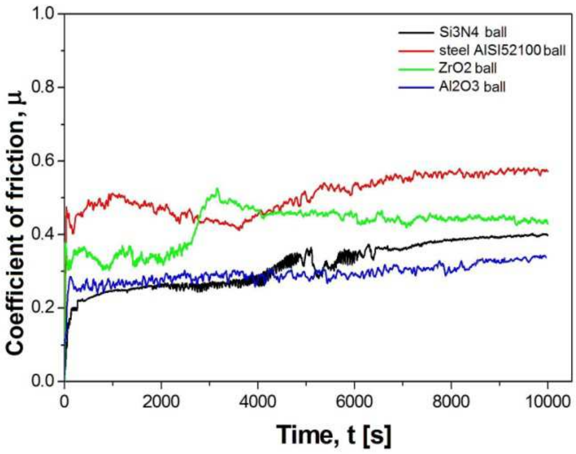

Fig. 2. Typical COF curves of: a) 316L steel, b) 316L steel+5% TiB_2 and c) 316L steel+10% TiB_2 as function of testing time, measured using different balls

Rys. 2. Współczynnik tarcia: a) stali 316L, b) kompozytu stal 316L+5% TiB_2, c) kompozytu stal 316L+10% TiB_2 w funkcji czasu testu, zmierzony przy zastosowaniu różnych kulek (przeciwpróbek)

TABLE 3. **Weight loss, coefficient of friction and specific wear rate of sintered steel and composites**

TABELA 3. **Wyniki badań ubytku masy, współczynnika tarcia i wskaźnika zużycia dla spiekanych kompozytów i stali 316L**

Sample	Ball	Mass loss m [g]	Relative weight loss Δm [%]	Specific wear rate $\cdot 10^{-6}$ W_a [mm^2/Nm]	Coefficient of friction μ [-]
316L steel	Al_2O_3	0.0319	1.45	823.23	0.55
	Si_3N_4	0.0290	1.06	748.39	0.58
	ZrO_2	0.0234	0.89	603.87	0.55
	steel	0.0131	0.17	338.06	0.70
316L steel + 5%TiB_2	Al_2O_3	0.0221	0.65	593.29	0.40
	Si_3N_4	0.0208	0.57	558.23	0.48
	ZrO_2	0.0167	0.50	448.32	0.48
	steel	0.0091	0.09	244.30	0.62
316L steel+ 10%TiB_2	Al_2O_3	0.0171	0.53	482.37	0.37
	Si_3N_4	0.0153	0.44	431.59	0.41
	ZrO_2	0.0140	0.45	394.92	0.43
	steel	0.0071	0.05	200.28	0.59

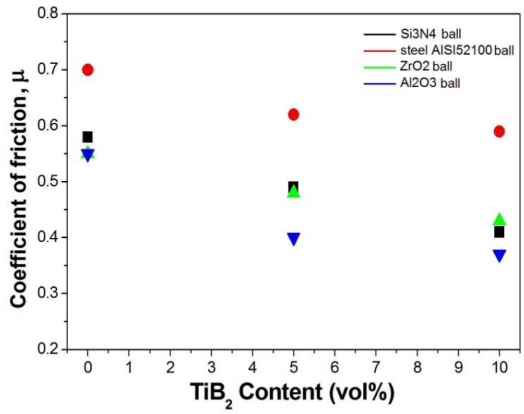

Fig. 3. Coefficient of friction as function of TiB_2 content, measured using different balls

Rys. 3. Współczynnik tarcia w funkcji zmiany zawartości TiB_2, zmierzony przy zastosowaniu różnych kulek (przeciwpróbek)

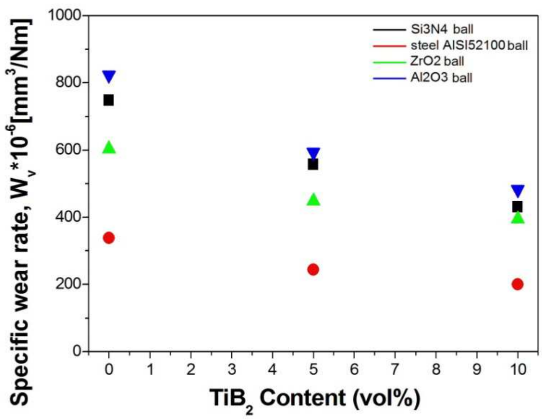

Fig. 4. Variation of specific wear rate as function of TiB_2 content, measured using different balls

Rys. 4. Zmiana wskaźnika zużycia w funkcji zmiany zawartości TiB_2, zmierzona przy zastosowaniu różnych kulek (przeciwpróbek)

Images of the composite surfaces after the tribological tests using different counter-samples (Al_2O_3, Si_3N_4 and ZrO_2) are shown in Figures 5-7. The examined surfaces bear traces of adhesive and abrasive wear. In the wear track zone, as a result of the tribological tests, protrusions and irregularities on the surface are first fused together and then sheared, which indicates the adhesive type of wear. This type of wear usually occurs at low speeds and high pressures, especially under conditions of dry friction when there is no lubrication. Adhesive wear is defined as a type of wear occurring on the surfaces of rubbing bodies as a result of the formation of local adhesive bonds which are then broken (destroyed) by metal particles that are detached or stuck to the surface [18, 27]. Figures 5-7 show traces of wear as a result of fusion of the 1st type. During the tribological tests, fusing of the ball and disc materials took place, followed by decohesion of the steel. Some fragments of the bridge of fusion remaining on the ball surface could make scratches on the sample surface.

a) b) c)

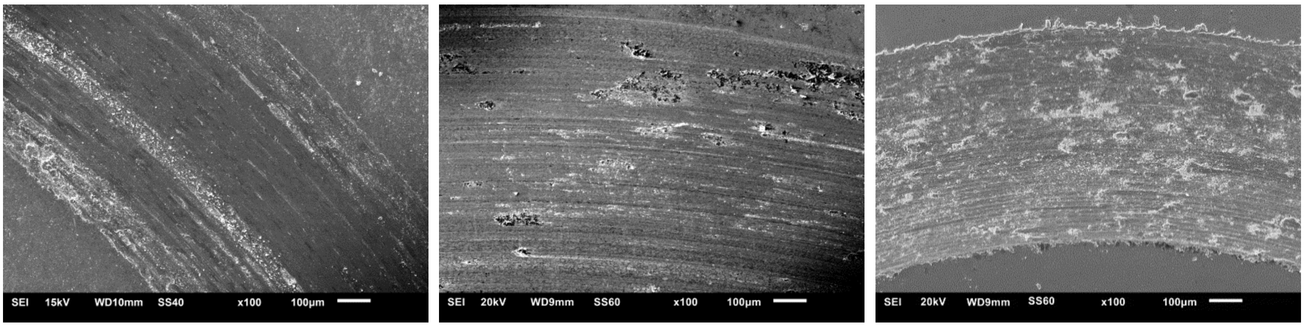

Fig. 5. View of 316L steel surface after rubbing against ball of: a) Al_2O_3, b) Si_3N_4, c) ZrO_2

Rys. 5. Widok powierzchni stali 316L po badaniach ścieralności z kulką: a) Al_2O_3, b) Si_3N_4, c) ZrO_2

a) b) c)

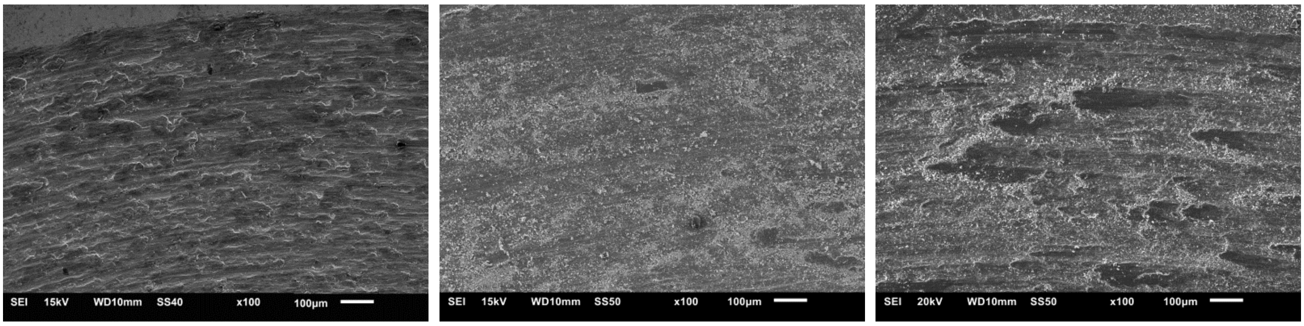

Fig. 6. View of surface of 316L steel+5%TiB_2 composites after rubbing against ball of: a) Al_2O_3, b) Si_3N_4, c) ZrO_2

Rys. 6. Widok powierzchni kompozytu stal+5%TiB_2 po badaniach ścieralności z kulką: a) Al_2O_3, b) Si_3N_4, c) ZrO_2

a) b) c)

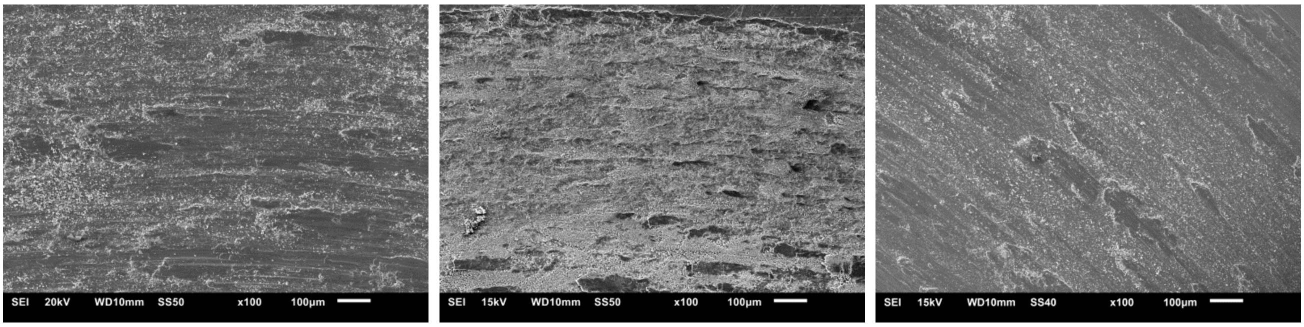

Fig. 7. View of surface of 316L steel+10%TiB_2 composites after rubbing against ball of: a) Al_2O_3, b) Si_3N_4, c) ZrO_2

Rys. 7. Widok powierzchni kompozytu stal+10%TiB_2 po badaniach ścieralności z kulką: a) Al_2O_3, b) Si_3N_4, c) ZrO_2

Figures 8-10 show micrographs of the ball surface after tribological testing of the 316L steel + 10% TiB_2 composites. Material worn off the tested sample (steel matrix) was observed on all the surfaces of the ceramic balls. After the tribological tests, there were no signs of wear on the surfaces of the Al_2O_3 or Si_3N_4 balls (Figs. 9 and 10). Visible traces of wear were observed only on the surface of the ball made of ZrO_2 (Fig. 8). The hardness of Al_2O_3, Si_3N_4 and ZrO_2 is 2200 HV, 2100 HV and 1300 HV, respectively [25]. Ceramic materials based on ZrO_2 are characterized by the lowest hardness, which can affect the surface wear of the ball.

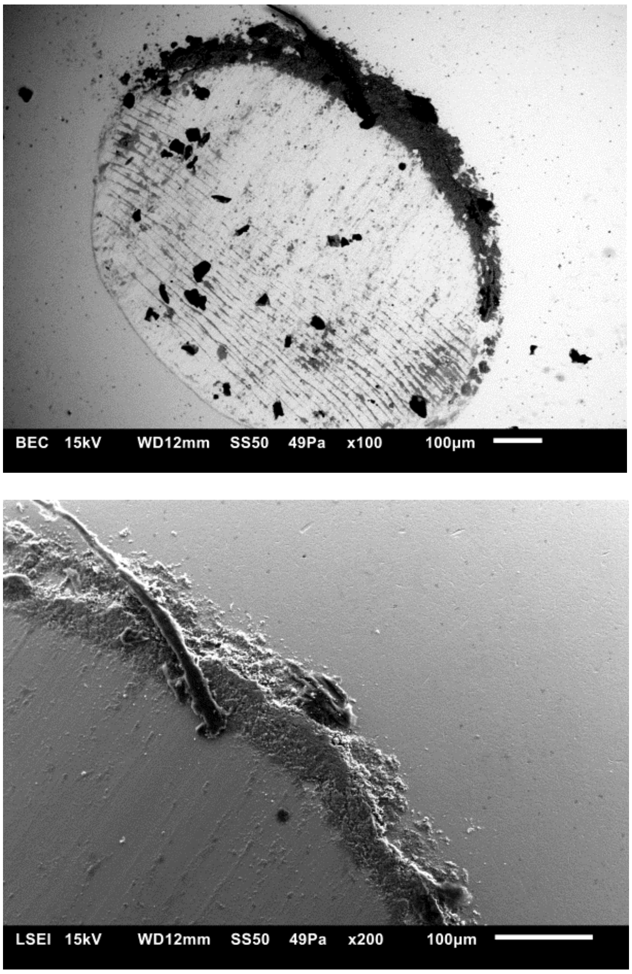

Fig. 8. Microphotographs of ZrO_2 ball after tribological test

Rys. 8. Mikrofotografia powierzchni kulki ZrO_2 po testach tribologicznych

In the case of sintered composites, the second mechanism that intensifies the wear process may be adhesive wear, as evidenced by scratches and furrows in the wear track zone (Figs. 6 and 7). Their presence may be due to the effect of tearing the reinforcing phase (TiB_2) out of the matrix and loose transfer of ceramic particles along the wear track (between the sample and counter-sample contact surfaces). The transferred ceramic particles can scratch the surface of the cooperating sample or cause plastic deformation of the matrix.

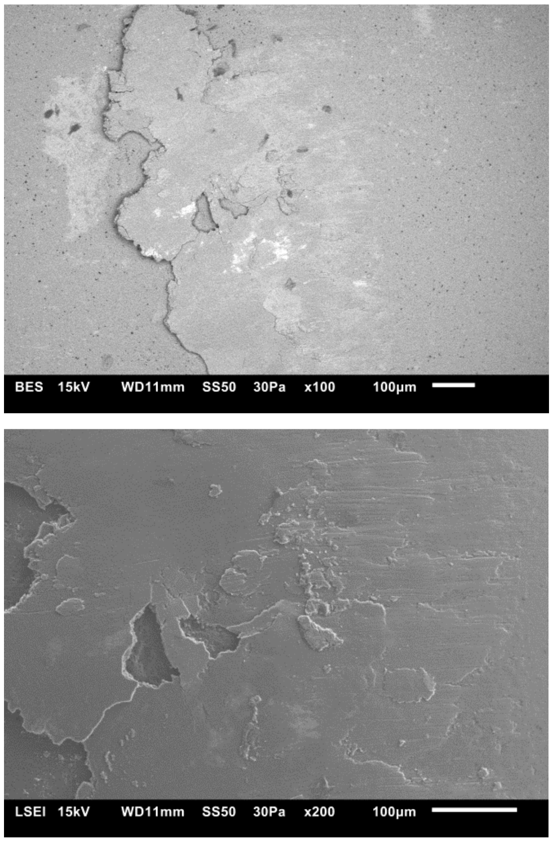

Fig. 9 Microphotographs of Al_2O_3 ball after tribological test

Rys. 9. Mikrofotografia powierzchni kulki Al_2O_3 po testach tribologicznych

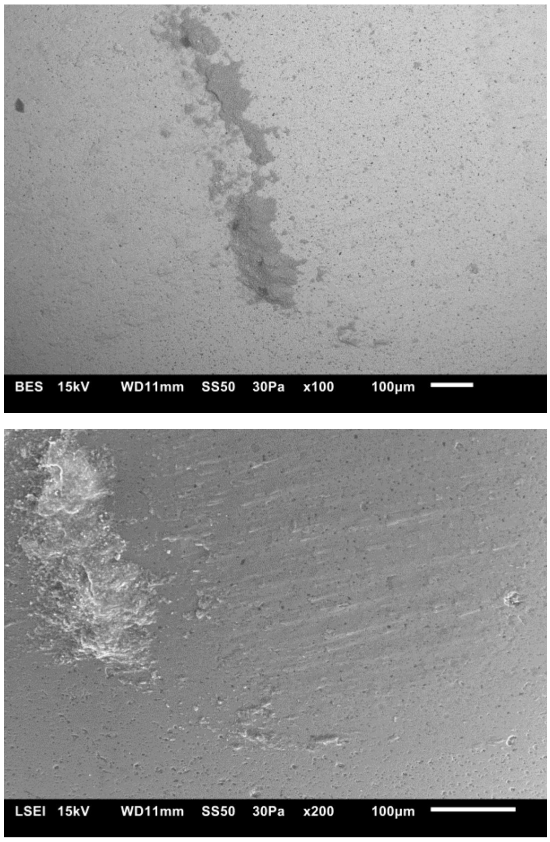

Fig. 10. Microphotographs of Si_3N_4 ball after tribological test

Rys. 10. Mikrofotografia powierzchni kulki Si_3N_4 po testach tribologicznych

CONCLUSIONS

The tribological behaviour of 316L steel+TiB_2 composites was studied by the ball-on-disc method. The increase in TiB_2 content improves the physical and mechanical properties of the composites. It also has a beneficial effect on the wear resistance. The coefficient of friction and the wear rate decrease with the increasing content of TiB_2 particles. The use of steel balls and ceramic balls made of Al_2O_3, Si_3N_4 and ZrO_2 in the tribological tests allowed different values of the coefficient of friction and wear rate to be obtained from the examined materials. The wear mechanisms were adhesive and abrasive in all the examined materials.

Acknowledgements

The study was conducted thanks to statutory funds of the Faculty of Mathematics, Physics and Technical Science, Pedagogical University of Cracow.

REFERENCES

[1] Lis J., Pampuch R., Spiekanie, Uczelniane Wydawnictwa Naukowo-Dydaktyczne AGH, Kraków 2000.

[2] Nowacki J., Spiekane metale i kompozyty z osnową metaliczną, Wydawnictwo Naukowo-Techniczne, Warszawa 2005.

[3] Ibrahim I., Mohamed F., Lavernia E., Particulate reinforced metal matrix composites - a review, Journal of Materials Science 1991, 26 (5), 1137-1156.

[4] Ghasali E., Pakseresht A. H., Alizadeh M., Shirvanimoghaddam K., Ebadzadeh T., Vanadium carbide reinforced aluminum matrix composite prepared by conventional, microwave and spark plasma sintering, Journal of Alloys and Compounds 2016, 688, 527-533.

[5] Borkar T., Nag S., Ren Y., Tiley J., Banerjee R., Reactive spark plasma sintering (SPS) of nitride reinforced titanium alloy composites, Journal of Alloys and Compounds 2014, 617, 933-945.

[6] Mukherjee S.K., Upadhyaya G.S., Corrosion behaviour of sintered 434L ferritic stainless steel-Al_2O_3 composites containing phosphorus, Corrosion Science 1985, 25(7) 463--470.

[7] Matejicek J., Boldyryeva H., Brozek V., Sachr P., Chraska T., Pala Z., W-steel and W-WC-steel composites and FGMs produced by hot pressing, Fusion Engineering and Design 2015, 100, 364-370.

[8] Darabara M., Papadimitriou G.D., Bourithis L., Tribological evaluation of Fe-B-TiB_2 metal matrix composites, Surface and Coatings Technology, 2007, 202(2), 246-253.

[9] Marshall P., Austenitic Stainless Steels: Microstructure and Mechanical Properties, Elsevier Applied Science Publishers, New York 1984.

[10] Ashok S.K., Das K., The abrasive wear resistance of TiC and (Ti,W)C-reinforced Fe-17Mn austenitic steel matrix composites, Tribology International 2010, 43(5-6), 944--950.

[11] Sulima I., Boczkal G., Micromechanical, high-temperature testing of steel-TiB_2 composite sintered by High Pressure--High Temperature method, Materials Science and Engineering A 2015, 644, 76-78.

[12] Zhang Z., Chen Y., Zhang Y., Gao K., Zuo L., Qi Y., Tribology characteristics of ex-situ and in-situ tungsten carbide particles reinforced iron matrix composites produced by spark plasma sintering, Journal of Alloys and Compounds 2017, 704, 260-268.

[13] Tjong S.C., Lau K.C., Abrasion resistance of stainless-steel composites reinforced with hard TiB_2 particles, Composites Science and Technology 2000, 60(8), 1141-1146.

[14] Riedel R., Handbook of Ceramic Hard Materials, WILEY-VCH Verlag GmbH 2000, 2, 968-990.

[15] Rao J., Cruz R., Lawson K.J., Nicholls J.R., Carbon and titanium diboride (TiB_2) multilayer coating, Diamond and Related Materials 2004, 13, 2221-2225.

[16] Matkovich V.I., Boron and Refractory Borides, Springer Berlin 1977, 172.

[17] Gierek A., Zużycie tribologiczne, Wydawnictwo Politechniki Śląskiej, Gliwice 2006.

[18] Płaza S., Margielewski L., Celichowski G., Wstęp do tribologii i tribochemia, Wydawnictwo Uniwersytetu Łódzkiego, Łódź 2005.

[19] Akhtar F., Microstructure evolution and wear properties of in situ synthesized TiB_2 and TiC reinforced steel matrix composites, Journal of Alloys and Compounds 2008, 459, 491-497.

[20] Wang Z., Lin T., He X., Shao H., Tang B., Qu X., Fabrication and properties of the TiC reinforced high-strength steel matrix composite, International Journal of Refractory Metals and Hard Materials 2016, 58, 14-21.

[21] Tjong S.C., Lau K.C., Sliding wear of stainless steel matrix composite reinforced with TiB_2 particles, Materials Letters 1999, 41, 153-158.

[22] Tjong S.C., Lau K.C., Abrasion resistance of stainless-steel composites reinforced with hard TiB_2 particles, Composites Science and Technology 2000, 60, 1141-1146.

[23] International Standard, Fine ceramics (advanced ceramics, advanced technical ceramics) - Determination of friction and wear characteristics of monolithic ceramics by ball-on-disc method, ISO 20808:2004(E).

[24] Meozzi M., Special use of the ball on disc standard test, Tribology International 2006, 39, (6), 496-505.

[25] Somija S., Handbook of Advanced Ceramics: Materials, Applications, Processing and Properties, Oxford 2013.

[26] PN-EN ISO 683-17:2015-01 - wersja angielska, Stale do obróbki cieplnej, stale stopowe i stale automatowe - Część 17: Stale na łożyska kulkowe i wałeczkowe.

[27] Lawrowski Z., Tribologia. Tarcie, zużywanie i smarowanie, Oficyna Wydawnictwa Politechniki Wrocławskiej, Wrocław 2008.

